Wintertime spatial characteristics of boundary layer aerosols over peninsular India

K. Krishna Moorthy,[1] S. V. Sunilkumar,[1] Preetha S. Pillai,[1] K. Parameswaran,[1] Prabha R. Nair,[1] Y. Nazeer Ahmed,[2] K. Ramgopal,[2] K. Narasimhulu,[2] R. Ramakrishna Reddy,[2] V. Vinoj,[3] S. K. Satheesh,[3] K. Niranjan,[4] B. Malleswara Rao,[4] P. S. Brahmanandam,[4] Auromeet Saha,[5] K. V. S. Badarinath,[6] T. R. Kiranchand,[6] and K. Madhavi Latha[6]

Received 15 October 2004; revised 27 December 2004; accepted 21 January 2005; published 30 April 2005.

[1] During an intense field campaign for generating a spatial composite of aerosol characteristics over peninsular India, collocated measurements of the mass concentration and size distribution of near-surface aerosols were made onboard instrumented vehicles along the road network during the dry, winter season (February–March) of 2004. The study regions covered coastal, industrial, urban, village, remote, semiarid, and vegetated forestlands. The results showed (1) comparatively high aerosol (mass) concentrations (exceeding 50 $\mu g\ m^{-3}$), in general, along the coastal regions (east and west) and adjacent to urban locations, and (2) reduced mass concentration (<30 $\mu g\ m^{-3}$) over the semiarid interior continental regions. Fine, accumulation-mode particles (<1 μm) contribute more than 50% to the total aerosol mass concentration in the coastal regions, which is more conspicuous along the east coast than the west coast, while the interior regions showed abundance (>50% of the total) of coarse-mode aerosols (>1 μm). The spatial composite of accumulation-mode share to the total aerosol mass concentration agreed very well with the monthly mean spatial composite of aerosol fine-mode fraction for February 2004, deduced from Moderate-Resolution Imaging Spectroradiometer data for the study region, while a point by point comparison yielded a linear association with a slope of 1.09 and correlation coefficient of 0.79 for 76 independent data pairs. Pockets of enhanced aerosol concentration were observed around the industrialized and urban centers along the coast as well as inland. Aerosol size distributions were parameterized using a power law. Spatial variation of the retrieved aerosol size index shows relatively high values (>4) along the coast compared to interior continental regions except at a few locations. Urban locations showed steeper size spectra than the remote locations.

Citation: Moorthy, K. K., et al. (2005), Wintertime spatial characteristics of boundary layer aerosols over peninsular India, *J. Geophys. Res.*, *110*, D08207, doi:10.1029/2004JD005520.

1. Introduction

[2] Atmospheric aerosols, particularly those near the surface, have strong direct and indirect influence on the environment, air quality, visibility and human health with immediate repercussions, while they alter the radiation budget of the Earth-atmosphere system through radiative forcing thereby affecting the climate on a long-term scale [*Charlson and Rodhe*, 1982; *Charlson et al.*, 1992; *Boucher and Anderson*, 1995]. Even though the significance of aerosols in these processes are globally recognized and several efforts have been made to model their characteristics from the above perspective, there still exists large uncertainties not only globally [*Penner et al.*, 2001] but also regionally [*Ramanathan et al.*, 2001; *Moorthy et al.*, 2001, 2003]. This arises mainly because of the large heterogeneity (spatial and temporal) in their properties (physical and chemical composition) and lack of experimental data with adequate spatiotemporal resolution. Near the surface, where the boundary layer process are active, the variabilities in aerosol characteristics are considerably higher, primarily because of the large diversity in the sources and sinks of aerosols, their short atmospheric residence time and also transport processes [*Pillai and Moorthy*, 2001; *Moorthy et al.*, 2003; *Väkevä et al.*, 2000]. Besides, advection by

[1]Space Physics Laboratory, Vikram Sarabhai Space Centre, Trivandrum, India.
[2]Department of Physics, Sri Kirshnadevaraya University, Anantapur, India.
[3]Centre for Atmospheric and Oceanic Sciences, Indian Institute of Sciences, Bangalore, India.
[4]Department of Physics, Andhra University, Visakhapatnam, India.
[5]Aryabhatta Research Institute for Observational Sciences, Uttaranchal, India.
[6]Forestry and Ecology Division, National Remote Sensing Agency, Hyderabad, India.

0148-0227/05/2004JD005520$09.00

synoptic winds, mesoscale land/sea breeze circulation and aging processes such as coagulation, humidification, scavenging by precipitation and gas to particle conversion modify the aerosol system both over the land and ocean [e.g., *Smirnov et al.*, 2002].

[3] To characterize this diversity, there have been a flurry of field experiments in the last decade: Smoke, Clouds, Aerosols and Radiation-Brazil (SCAR-B) for studying the radiative impacts, smoke and aerosols form the biomass burning in Brazil [*Kaufman*, 1998]; Troposphere Aerosol Radiative Forcing Experiment (TARFOX) for characterizing the eastern U.S. emission into Atlantic and their radiative impacts [*Russell et al.*, 1999]; Aerosol characterization experiment (ACE-I) in pristine remote marine atmosphere, south of Australia [*Bates et al.*, 1998] and ACE-II, anthropogenically modified atmosphere of the eastern Atlantic (European plume, African dust plume) [*Raes et al.*, 2000]; Indian Ocean Experiment (INDOEX) to assess the radiative impacts of the heavily mixed aerosols over the Indian Ocean [*Ramanathan et al.*, 2001]); and most recently the ACE-Asia, conducted off the coast of east China, Korea, and Japan with a view to understanding the anthropogenically modified aerosol environments of east Asia and their impact on regional radiative forcing [*Huebert et al.*, 2003]. However, in these campaigns primary focus was mostly on oceanic environments, which are less heterogeneous than the landmass. Field studies focusing on spatial variation of aerosol characteristics over the land are rather limited and difficult even though it constitutes to most of the uncertainty in impact assessment. Several experimental efforts have been made recently making use of road networks and instrumented vehicles. Most of these road campaigns, conducted at different environments, such as urban, rural, coastal and marine locations of Netherlands [*Weijers et al.*, 2004], urban and rural areas of Rouen, France [*Gouriou et al.*, 2004], urban, rural and background sites in Europe [*Dingenen et al.*, 2004], and urban and rural locations of Switzerland [*Bukowiecki et al.*, 2002], were, however, more focused toward understanding pollution related to traffic emissions and most of these observations were conducted close to the source regions, whereas "far-field" measurements are more appropriate for modeling aerosols for regional/global radiative impact assessment. Over the Indian landmass, studies focusing on the spatial heterogeneity of aerosol properties are scarce, notwithstanding its high density of population, increasing industrialization and urbanization, diverse living habits, geographical features and contrasting meteorological processes. However, such data are essential to assess the regional radiative forcing and also to delineate the temporal changes. With the above considerations an intense land campaign was conceived for spatial mapping of aerosol characteristics over peninsular India during the winter season (February–March) under the Indian Space Research Organisation's Geosphere Biosphere Programme (I-GBP). Such a campaign, with a number of research teams participated using instrumented vehicles along the road network covering different geographical locations, was carried out for the first time in this region. During this, the peninsular India was almost completely covered by four teams (designated hereafter as T1, T2, T3 and T4). The results from these measurements, described in this paper, are expected to provide significant input for developing regional aerosol models for radiative forcing estimates.

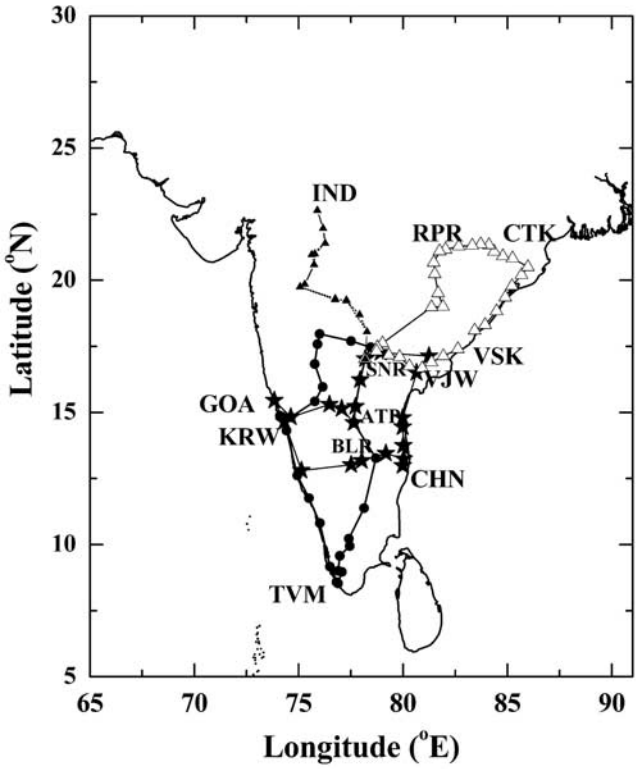

Figure 1. Route map followed by the teams during the campaign. The points on the respective track lines identify the geographical locations where observations were made.

2. Experimental Details

[4] The campaign was conducted during the period 1 February 2004 to 2 March 2004 continuously for 31 days during which the four teams made measurements of aerosol characteristics simultaneously over spatially separated locations using identical or nearly identical instruments, carried in four instrumented vans, along the route map shown in Figure 1. The track with circles shows the route covered by T1 (Space Physics Laboratory, Trivandrum), track with stars shows the route covered by T2 (Sri Krishnadevaraya University, Anantapur and Centre for Atmospheric and Oceanic Sciences, Bangalore), track with open triangles shows the route covered by T3 (Andhra University, Visakhapatnam) and track with filled triangles shows the route covered by T4 (National Remote Sensing Agency, Hyderabad). The points on the respective track lines identify the geographical locations where observations were made. The teams together covered a route length of about 15,000 km, making independent observations at 83 distinct locations covering coastal, inland, arid, urban, and plateau regions. A digital elevation map of the study region is given in Figure 2, which shows that the coastal regions covered were at low elevation <100 m msl), while most of the inland plateau region were 150 to 600 m msl and few locations were >1.5 km altitude. The month of February has been specifically chosen for this campaign because during

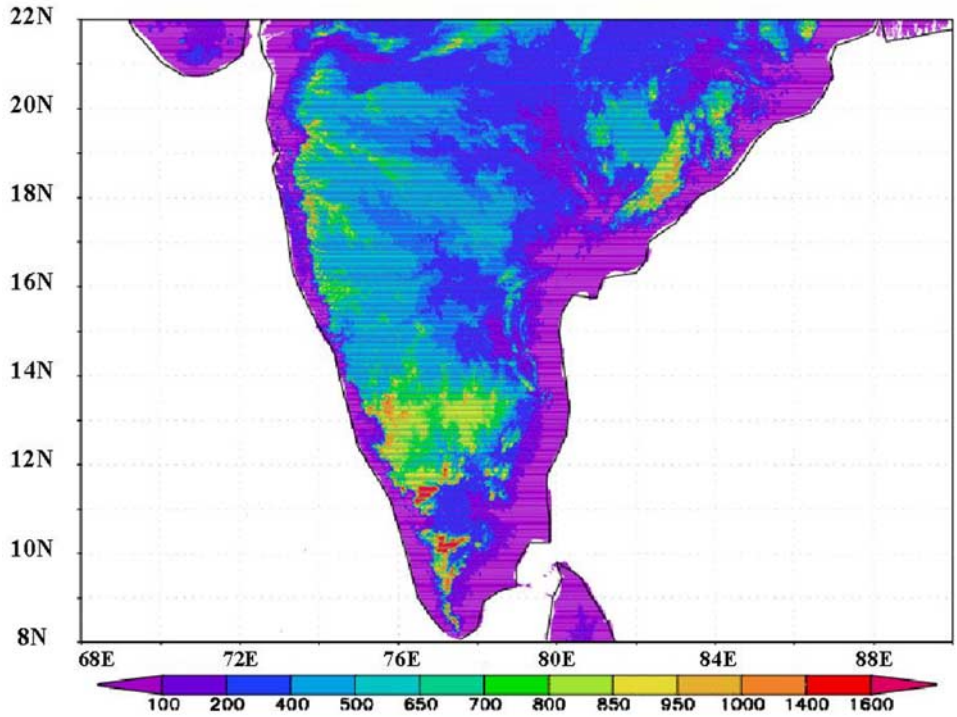

Figure 2. Digital elevation model of south India showing the terrain details.

this period wet removal processes are almost absent over Peninsular India providing a longer residence time for aerosols in the atmosphere. This period is also devoid of any major weather phenomena, so that the temporal changes are far less pronounced than in other seasons.

2.1. Synoptic and Local Meteorology

[5] During the campaign period surface winds were, in general, calm to moderate (<3 m s^{-1}) with clear skies and no rainfall anywhere enroute. The mean prevailing wind patterns at 850 and 925 hPa for February 2004 over the Indian subcontinent, obtained from the National Centers for Environmental Prediction/National Center for Atmospheric Research (NCEP/NCAR) reanalysis data [*Kalnay et al.*, 1996] are shown in Figures 3a and 3b, respectively. The prevailing winds are generally weak (<3.5 m s^{-1}) easterly/northeasterly over most of the land including the eastern coast; they change to weak northerlies near the western coast at 925 hPa level, while they continue to be easterlies at 850 hPa.

[6] The surface relative humidity (RH) and temperature were measured enroute using thermohygrometers, wind speed using a hand-held anemometer and columnar water vapor content (W) (g cm^{-2}) using a Microtops Sun photometer instrument (Solar Light Company). Spatial variations of RH and T and W are shown in Figures 4a and 4b, respectively. The coastal regions (east/west) were generally humid, with high RH (in excess of 50%) while the inland, plateau regions were dry with the RH value dropping to (10 to 25%). Not only the surface RH, but column water vapor content also showed similar behavior (Figure 4b) with high values (2 to 3 cm) along the coast and very low (0.5 to 1.0 cm) in the inland regions. Surface winds were generally calm to weak (1 to 3 m s^{-1}) at almost all the locations, inline with prevailing winds except at one or two locations along the west coast where it went up to 6 m s^{-1}. The daytime surface temperatures (Figure 4a) were moderate (~30°C) along the coastal regions and high (>32°C) in the interior plateau regions to the south of 18°N, while lower values were observed farther north.

2.2. Aerosol Measurements

[7] A number of instruments were used to characterize the near-surface aerosols during the campaign, as detailed in Table 1. A brief description of the instruments, principle, sampling protocols, and site description are given below.

2.2.1. Quartz Crystal Microbalance Impactor (QCM)

[8] The QCM (model PC-2 California Measurements, Inc.) provided near-real-time measurements of the total, as well as size segregated aerosol mass concentration in the size range 0.05 to 25 μm resolved into 10 size bins. The 50% lower cutoff of each stage is given in terms of particle diameters derived from the aerodynamic diameter taking the particle density as 2 g cm^{-3}. Its pump aspirates the ambient air at a flow rate of 0.24 L min^{-1} and is sampled for a duration varying between 240 and 360 s depending on the particle concentration at the sampling location such that the frequency shift in the stages registering low mass concentration is ~5 Hz. Samples were collected at an interval of 30 to 60 min during the data collection period, so that each location/day had a minimum of 4 and a maximum of up to 15 samples. More details on the instrument, operating conditions and error budget are given in an earlier paper [*Pillai and Moorthy*, 2001].

2.2.2. High-Volume Sampler (HVS)

[9] Direct sampling of bulk aerosols near the surface has been made using a single-stage high-volume sampler (Model Handi-Vol GH 2000 of Graseby Anderson, USA). Quartz fiber discs of 4 inch diameter have been used as the

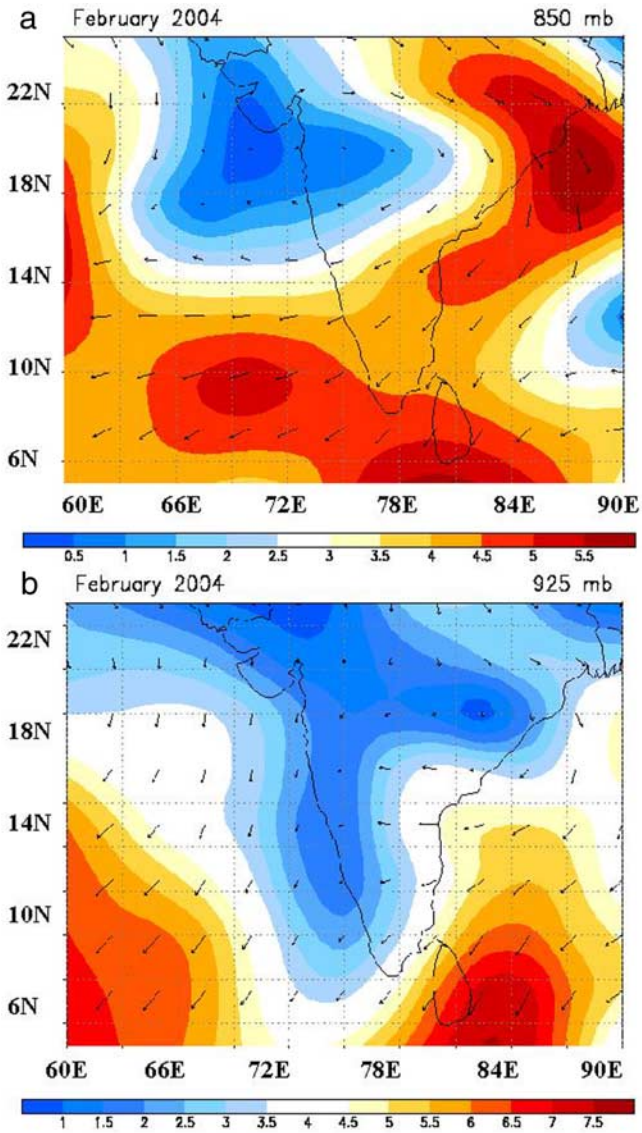

Figure 3. Mean isotachs (m s^{-1}) at (a) 850 and (b) 925 hPa level over Indian Peninsula for February 2004 obtained from National Centers for Environmental Prediction/ National Center for Atmospheric Research (NCEP/NCAR) reanalysis.

collection substrate. The mean flow rate was 567 L min^{-1} (20 CFM) and the calibration was ensured before and after the campaign period using the calibration set up. The quartz fiber substrates were preheated in an oven to 100°C and then desiccated for 24 hours. These substrates were then tare weighed using a microbalance (Model AT 120, Metler) with a precision of ±2 μg and sealed in separate numbered self-locking envelopes. Tare weighed substrate from the envelope is mounted on the impactor and aerosols samples are collected by operating it for a duration 3 to 4 hours at the sampling location. After sampling, substrates were sealed in the respective envelopes. In the laboratory these are desiccated for 24 hours and then are weighed using the same balance in the same room conditions. The difference between the final and tare weights gave the aerosol mass

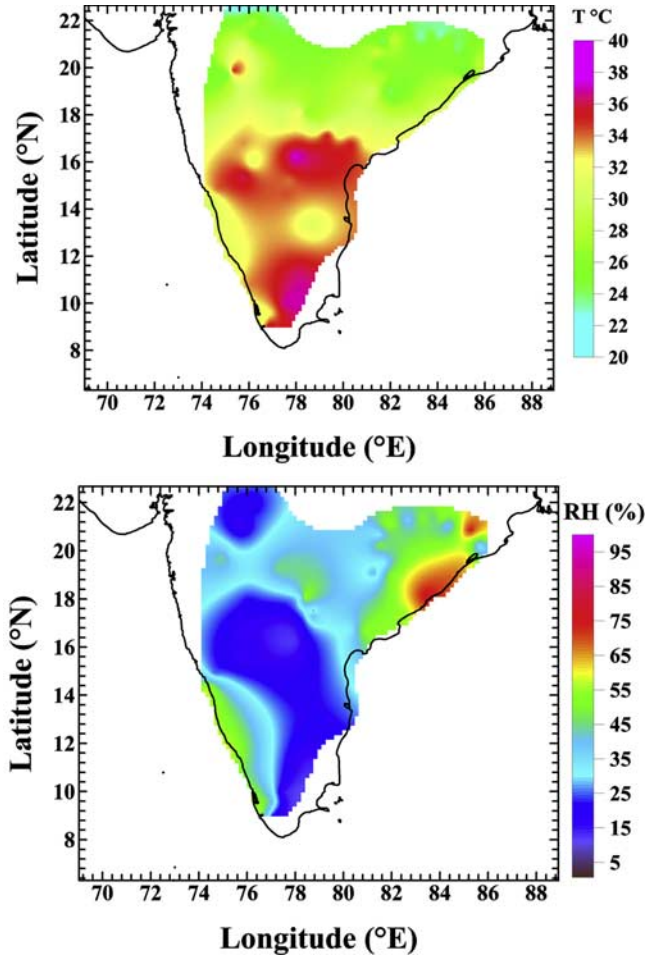

Figure 4a. Spatial variations of (top) ambient temperature and (bottom) surface relative humidity.

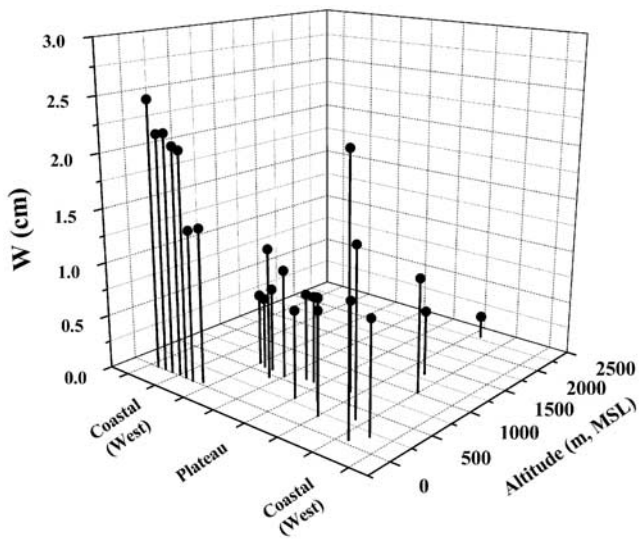

Figure 4b. Spatial variations of columnar water vapor content for the stations covered by team 1.

Table 1. Details of Instruments Used in This Study

Instrument Details[a]	Teams[b] 1	2	3	4	Parameters Measured
QCM	yes	yes	yes	yes	mass concentration and mass size distribution (0.05 to 25 μm)
HVS	yes				bulk mass concentration
Met-Sensors	yes	yes	yes	yes	relative humidity, temperature, and columnar water vapor

[a]QCM is Quartz Crystal Microbalance Impactor; HVS is high-volume sampler.
[b]Entry "yes" indicates the instrument was used by the team.

loading. Knowing the volume of air sampled (the flow rate times sampling duration), the mass concentration was estimated.

2.3. Measurement Protocols

[10] As the measurements were being carried out along the road network through a heterogeneous landscape of highly varying geographical properties and anthropogenic and/or urban activities, independently by different teams, it was essential to follow a common protocol. This was also necessitated by the physical considerations that near-surface aerosols are subjected to significant diurnal variations in their concentration and size distribution [e.g., *Pillai and Moorthy*, 2001] associated with diurnal variations in the characteristics of the atmospheric boundary layer and other mesoscale process such as land/sea breeze in a coastal environment. Considering all the above and the typical sunrise/sunset times (between 0640 and 0700 LT and between 1700 LT and 1730 LT, respectively) for the study region, the window of sampling was fixed to be between 0900 and 1630 LT. During this period, generally the boundary layer is well evolved and the morning fumigation effects are smoothed off, and the sea breeze would have set in at coastal areas. These conditions continue more or less the same way till around 1630 LT. Sampling sites were selected to be remote areas, typically 2 to 5 km away from any major roads and at least 500 m upwind of even minor roads or pathways. Generally, one location was sampled during each day. However, the sampling duration varied between 4 and 7 hours depending on the selection of an appropriate site. The distance between consecutive sites was about 150 km. Observations using QCM, Microtops, and meteorological sensors were made at every 30 min, while the HVS was operated only at a few locations where sufficient electrical power was available for longer duration.

2.4. Sampling Sites, Description, and Schedule

[11] The sampling sites covered coastal, inland, arid, urban and plateau regions as can be seen from Figures 1 and 2. Following Figure 1, T1 started from Trivandrum (TVM) (Figure 1, 8.5°N, 77°E) and traveled along the west coast till Karwar (KRW) (14.9°N, 74.1°E) before deviating to the inland vegetated forest regions, followed by the dry semiarid locations until 17.97°N, 76°N before moving southward to reach Shadnagar (SNR) (17.03°N, 78.19°E), which was selected as a common meeting point for all the teams to intercompare their measurements. T2 started from the urban city Bangalore (BLR) (13.02°N, 77.52°E) and moved eastward making measurements along the east coast till Nellore (14.45°N, 79.98°E), moved through the urban location Vijayawada (VJW) (16.5°N, 80.65°E), turned inland and reached SNR. T3 started from east coast urban location Visakhapatnam (VSK) (19.35°N, 84.9°E) moved north along the coast up to 21°N, then turned to the inland regions to reach SNR. T4 was confined only to the inland semi arid regions between 18° N to 23° N in the longitudinal sector 75 to 78° E. The instruments were intercompared at SNR by operating them simultaneously under similar ambient condition. Then the teams T1 and T2 returned to the original stations through the return path, through Central peninsular region until Anantapur (ATP) (14.61°N, 77.64°E). Form this location, T2 moved toward the west coast and made observations along the coast till Goa (GOA) (15.45°N, 73.83°E) and then moved toward BLR, whereas team 1 made observations toward the south and crossed Western Ghats (highest observation point Kodaikanal 2304 msl) and reached TVM. T3 moved toward the east and reached VSK. T4 completed the observations at SNR.

3. Analysis of Data

[12] During each measurement, the QCM provided direct information on (1) the total mass concentration (M_t) which is the mass of aerosols in the size range 0.05 to 25 μm in unit volume of the ambient air and (2) the mass concentration (m_{ci}) in each of its size bins (i = 1, 10) which provided the mass size distribution. These two parameters are directly related as

$$M_t = \sum_{i=1}^{10} m_{ci}. \quad (1)$$

The error in the measured mass concentration varies from 3 to 20% with the higher values for lower concentrations, following the details of error analysis and operation conditions given by *Pillai and Moorthy* [2001]. Accordingly, the uncertainty of the QCM stage radii due to the uncertainty in the assumed particle density is given as

$$\frac{\Delta r}{r} = -\frac{1}{2}\frac{\Delta \rho_p}{\rho_p}.$$

The density of aerosols is reported to vary from 1.8 to 3.0 g cm^{-3} from maritime to urban locations [*Hanel*, 1976; *Pruppacher and Klett*, 1978] and as such the value used in the QCM is well within the range.

[13] The individual estimates of M_t and m_{ci} (during each sampling) were averaged over the observation period of each day (as per the sampling protocol) to obtain the daily mean values, which correspond to the daytime period, when

Table 2a. Comparison of Total Aerosol Mass Concentration Obtained From Individual QCMs[a]

Date	T_1	T_2	T_3	T_4
16 Feb. 2004	NA	43.22 ± 4.25	36.04 ± 5	46.64 ± 4.52
17 Feb. 2004	31.72 ± 0.296	32.15 ± 1.71	31.21 ± 3	NA
19 Feb. 2004	36.94 ± 0.458	37.8 ± 5.22	NA	44.95 ± 4.42
22 Feb. 2004	48.0 ± 0.377	62.5 ± 5.73	NA	NA

[a]NA indicates nonavailability of data, either because of the instrument being put off for crystal cleaning and recalibration or the respective team being not present.

the diurnal variations in these parameters are generally the least.

4. Results and Discussion

[14] Considering the aerosol characteristics obtained during the campaign as samples derived from a statistically, temporally stable spatial pattern, we have examined the spatial distribution of aerosol properties over southern peninsular India by assimilating all the measurements. The above assumption, though cannot be strictly true, particularly for near-surface aerosols, was still considered due to several reasons: (1) The sampling area was rather small, ~14° wide along the latitude and 10° in longitude. (2) The general meteorological and environmental conditions over the sampling locations were stable, with calm to moderate winds, clear skies and no rainfall. (3) The study area was devoid of any weather phenomena. (4) A common measurement protocol was followed at all the sampling locations (as explained in section 2.3. (5) Time of sampling was such that the boundary layer was well evolved [*Moorthy et al.*, 2004] so that the impact due to the diurnal variation in the boundary layer height will be minimal. The above considerations were by and large valid for the period as also was revealed from satellite observations to be discussed in section 4.3.

4.1. Intercomparison

[15] Before proceeding to present the composite picture evolved by assimilating the entire data, it is essential to examine the repeatability, reliability, consistency and interchangeability of the measurements made by the QCMs used by the four teams. This was ensured by performing detailed intercomparison both between the identical parameters estimated using identical instruments (QCMs) as well as identical parameters estimated using different instruments (QCM and HVS). This was done when the teams met at common measurement points enroute and under similar ambient conditions at SNR. The results for the total mass concentration (M_t) deduced from the QCM are given in Table 2a, which shows a generally good agreement between the different measurements (averaged over the duration fixed by the protocol) within the overall measurement uncertainty.

[16] Similarly, the total mass concentration (M_t) estimated from QCM and total suspended particulate matter (TSP) obtained from HVS of T1 were intercompared at locations where these two instruments were operated under nearly identical condition for the same duration and the results are given in Table 2b. Here the M_t measurements made using the QCM are averaged (time weighted) for the duration for which the HVS was operated. This means that

$$(M_t)_{QCM} = \left[\sum_{i=1}^{n} M_{ti}\Delta t_i \Big/ \sum_{i=1}^{n} \Delta t_i \right], \quad (2)$$

where Δt is the time interval between successive sampling at any given location during which the total mass concentration is M_{ti} and n is the total number of samples during the period for which the HVS was operated. A general agreement is seen despite the differences in cutoff diameters (the HVS has no upper size discrimination (cutoff size), whereas QCM collects particles below 25 μm diameter), except in one case where the HVS value was lower than the QCM estimate and this is due to the difference in the locations (at that site) from where these two instruments were operated (the HVS from a rooftop).

[17] The general agreement (within ~20%) between the mean mass concentrations obtained from different QCMs used by the four teams as well as that estimated by the QCM and HVS showed that the data can be mixed together fairly accurately to build the spatial composite by treating the individual measurements by each team as independent spatial samples.

Table 2b. Comparison of Total Aerosol Mass Concentration From HVS and QCM[a]

Date	HVS TSP, μg m^{-3}	QCM M_t, μg m^{-3}
1 Feb. 2004	53.6	53.3
6 Feb. 2004	56.2	66.3
15 Feb. 2004	53.5	40.7
16 Feb. 2004	76.4	67.6
16 Feb. 2004	62.20	51.0

[a]TSP is total suspended particulate matter; M_t is total mass concentration.

4.2. Spatial Variation of Aerosol Mass Concentration

[18] The spatial composite of the M_t over the peninsular India is generated based on the above considerations and is shown in Figure 5. Several interesting points emerge:

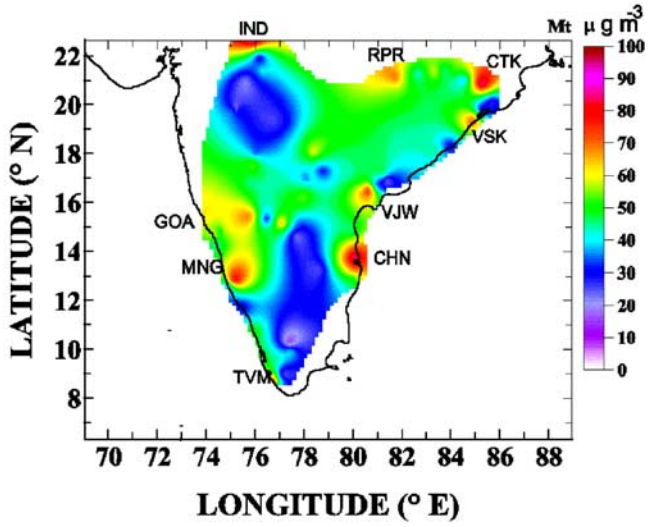

Figure 5. Spatial composite of total mass concentration (M_t).

[19] 1. The coastal areas, in general, have higher aerosol concentration (>50 $\mu g\ m^{-3}$). This is true for both the east and west coasts (except a few small pockets of low concentration appearing as blue). Compared to this, the inland regions have lower mass concentrations (<40 $\mu g\ m^{-3}$), despite these being nearly arid and totally dry, subjected to significant solar heating from the clear sky.

[20] 2. Over most of the coastal regions M_t varies from 50 to 80 $\mu g\ m^{-3}$, whereas M_t was <40 $\mu g\ m^{-3}$ over most of the inland regions in the south and west, dropping at times to as low as ~20 $\mu g\ m^{-3}$.

[21] 3. Hot spots of aerosol mass concentration >60 $\mu g\ m^{-3}$ are observed around urban locations such as TVM (8.53°N, 76.88°E), the regions around KRW, GOA (12.62°–15.5°N, 73.8°–74.6°E), along east coast from Chennai (CHN) (13.24°N, 80.03°E) to Vijayawada (VJW) (16.5°N, 80.65°E), around VSK (19.35°N, 84.9°E) and Cuttak (CTK) (20.8°N, 85.7°E), Raipur (RPR) (21.2°N, 81.6°E) and Indore (IND) (22.5°N, 72.76°E) in the inland regions. All these, except TVM, are industrialized urban centers with significant anthropogenic activities. Besides, MNG, GOA, CHN and VSK are major ports and have lot of related human activities.

[22] 4. It is also interesting to note that out of the eight hot spot regions, five are along the coastal belt.

[23] All these hot spots are clearly seen in Figure 5, despite the sampling was made quite far from the urban centers in accordance with the protocols. However, these hot spots are rather spatially confined and do not appear to spread. This might be indicative of the less efficient transport processes near the surface, because of the weak nature of winds. The high aerosol loading seen along the coastal regions could be attributed to several factors:

[24] 1. The population density is high, and there is a consequent anthropogenic impact. According to the recent estimates ~70% of the more than 1 billion population of India lives in the coastal belt, extending over 7500 km and the study region covered a major part of the Indian coastline. The coastal regions covered also had several semiurban centers with population of above 1 million. Though no data were collected in the urban proper, sampling locations around these centers even 20 to 30 km away still show the signature.

[25] 2. The coastal region covered had at least five major ports, two (CHN, VSK) on the east and three (GOA, MNG, and Cochin) on the west coast and several minor ports and fishing harbors, all these resulting in a substantial amount of anthropogenic activities and related emissions.

[26] 3. The RH is comparatively high. It can be seen from Figure 4a, that both RH and W were >3 to 4 times higher along the coastal region than the values encountered inland. This high humidity is conducive for growth of hygroscopic aerosols as well as formation of new particles by gas to particle conversion from the precursors emitted by the anthropogenic activities. The abundant sunlight available because of clear skies and proximity to equator and high water vapor content favor this.

[27] 4. The prevailing sea breeze activity results in a lower temperature and shallow thermal internal boundary layer (TIBL) at the coast [e.g., *Kunhikrishnan et al.*, 1993], which would limit the vertical mixing of aerosols in the coastal areas, resulting in confining the aerosols in a lesser spatial extent and leading to enhancement in near-surface concentration.

[28] 5. The sea-salt component is advected by the sea breeze [e.g., *Moorthy et al.*, 1993].

[29] 6. The convergence of the prevailing synoptic wind near the west coast (Figure 3b) due to a change in direction, from north easterly in the inland to northerly at the coast, leads to stagnation of aerosols causing an enhancement in surface concentration.

[30] 7. There is long-distance transport (by the prevailing winds) of fine aerosols from the central Indian region. Such transport of fine aerosols from continental regions to peninsular India and the oceanic regions has been reported earlier by *Ramanathan et al.* [2001], *Lelieveld et al.* [2001], and *Moorthy et al.* [2001].

[31] The observed high concentration along the western coastal locations is also in agreement with the earlier reports by several investigators during the Indian Ocean Experiment (INDOEX), conducted during February–March months of 1998 and 1999, which showed total aerosol mass concentration up to 80 $\mu g\ m^{-3}$ [*Jayaraman*, 1999; *Momin et al.*, 1999; *Pillai et al.*, 2002; *Parameswaran et al.*, 2004] along the coastal waters adjoining the western coast of India. It may also be recalled that not only the near-surface concentrations, but even the columnar optical depths also showed high values around GOA-MNG region during both the field phases of INDOEX [*Moorthy et al.*, 2001].

[32] The above scenario shifts significantly as we move to inland areas. The RH decreases drastically to 10–20% level. The density of population also reduced considerably and most of the regions covered were barren/dry agricultural land with sparsely inhabited villages. Though the arid land and dry atmospheric conditions are conducive for generation of coarse sandy aerosols, they are not in abundance because of the low wind speeds and near absence of anthropogenic activities such as vehicular transport. Yet the impact of urban region are seen near RPR (21.2°N, 81.6°E), Indore (22.5°N, 72.76°E), Hyderabad (18.05°N, 78.3°E), and BLR (13.02°N, 77.5°E) as small "hot spots." It should be borne in mind that as our aim was to characterize aerosols regionally and not to quantify the source strengths; the urban centers are not sampled at all. It is possible that the M_t would be much higher within the urban centers, but this was beyond the scope of the study.

[33] In view of the above and also keeping in mind that because of the distinct generation mechanisms of natural and anthropogenic aerosols (the former mostly by mechanical processes and the latter mostly due to secondary production mechanisms) we separated the aerosols into the accumulation-mode range ($d < 1\ \mu m$) and coarse-mode range ($d > 1\ \mu m$). The continental aerosols of mainly anthropogenic origin lie in the accumulation regime, while windblown dust and sea spray aerosols lie in the coarse regime. Soot from biomass burning and vehicular exhaust also mainly lies in the accumulation regime. Accumulation-mode particles are longer-lived and more amenable for long-distance transport while the coarse-mode particles having short lifetimes are only of local relevance. Hence it is very important to study the size differentiated spatial variation of aerosol mass concentration. Thus we estimated

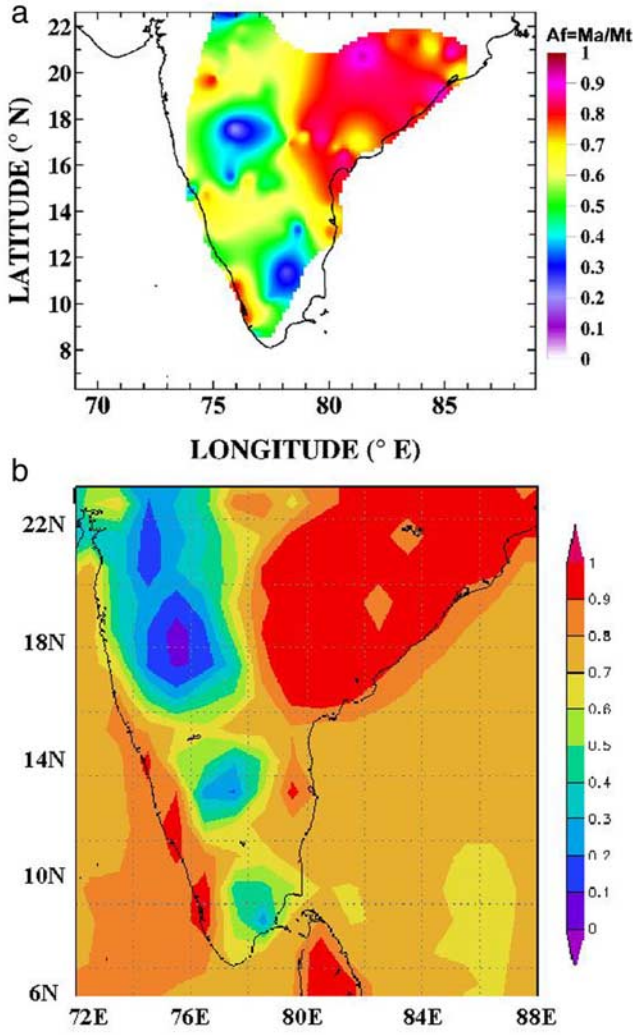

Figure 6. Spatial variation of (a) accumulation mass fraction and (b) Moderate-Resolution Imaging Spectroradiometer (MODIS)-derived fine-mode fraction.

the accumulation aerosol mass fraction or simply the accumulation fraction, A_f, as the ratio of M_a to M_t such that

$$A_f = \frac{M_a}{M_t}, \tag{3}$$

where M_a is the mass concentration of accumulation-mode aerosols estimated from the QCM measurements as

$$M_a = \sum_{i=7}^{10} m_{ci} \tag{4}$$

and M_t is given by equation (1). For the cutoff points of the QCM, the summation in equation (4) covers particles smaller than 0.8 μm in diameter. For each observation location, A_f is thus estimated and the spatial composite generated is shown in Figure 6a. It is readily seen that accumulation-mode aerosols contributed to more than 50% of the total aerosol mass concentration almost over the entire region except for some isolated pockets lying in the interior and elevated regions. Very large abundance exceeding 80% to the total mass concentration is seen in the eastern India bounded between 78°E and 86°E and 14°N and 22°N. Interestingly, such high abundances are seen only in some small pockets in the western coast. Nevertheless, M_a still accounts for ~70% of M_t in most of these regions. This pattern was consistent irrespective of the absolute value (M_t). Figure 6a also shows that the high accumulation fraction prevails not only along the coast (where M_t also was generally high) but high to very high accumulation fractions $\geq$ 0.8 are seen over inland regions, particularly toward the northern and eastern parts. In other words, most of the landmass surveyed had accumulation fraction exceeding 0.6, except the three regions in the central peninsula, adjoining the forested high lands and sparsely inhabited plateau regions where the A_f is 0.2 to 0.5. Dominance of accumulation-mode aerosols during winter has also been reported on the basis of long-term observations at the western coastal location TVM [*Pillai and Moorthy*, 2001].

4.3. Comparison of Accumulation Fraction With Satellite (MODIS) Derived From Fine-Mode Fraction

[34] We now proceed to compare the spatial variation of accumulation fraction, A_f, observed during this land campaign over peninsular India with fine-mode fraction (*ff*) derived from satellite (MODIS) for the same period. It is defined as fraction of aerosol concentration below 1 μm. In Figure 6b we show the monthly mean, 1°×1°, fine-mode fraction deduced from MODIS data (MODIS level – 3 product [*Kaufman et al.*, 1997]) for the month of February 2004 for the study region (7°N to 24°E, 72°E to 84°E). The resemblances in the spatial patterns between Figures 6a and 6b are remarkable. The extended highs in eastern and northern parts as well as the pockets of low in central western and southern peninsula appear almost identically in both. To make this comparison more quantitative, we made a one to one comparison between the accumulation fraction from our measurements (QCMs) with the monthly mean MODIS derived fine-mode fraction for the 1° × 1° grid point of MODIS closest to or around our observation locations. The results are shown in the scatterplot of Figure 7. The dotted line is the best fit to the scatterplot through the origin. It gives an empirical relation between the two of the form

$$ff = (1.09 \pm 0.023) A_f \tag{5}$$

with a correlation coefficient of 0.79, which is significant at $\rho < 0.0001$, for the 76 independent measurements. This agreement is quite good, in general, and remarkable, in particular, when we also consider the following:

[35] 1. MODIS-derived *ff* is retrieved from spectral aerosol optical depth (AOD) estimates and hence would correspond to columnar measurements while the QCM measurements are in situ and near the surface.

[36] 2. The MODIS data are the mean for February, while the QCM data are averages of daily spot measurements. However, the remarkable agreement between the two renders validity to our consideration that the temporal variability in aerosol properties were rather small in February and the spatial composite almost represents the mean pattern for the region of the month, rending further support to the selection of the campaign period.

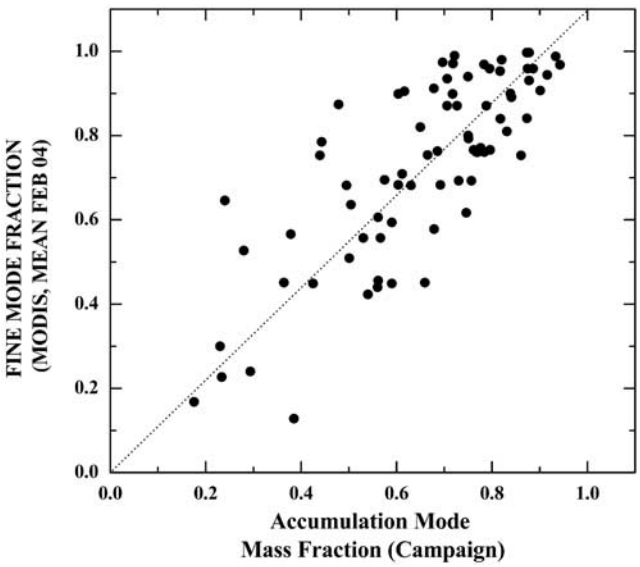

Figure 7. Scatterplot of MODIS-derived fine-mode fraction and accumulation-mode mass fraction estimated from ground measurements. The dotted line is least squares fitted through the origin.

[37] 3. The MODIS-retrieved fraction is related to number concentration, while the QCM-derived fraction corresponds to mass concentration.

[38] If the accumulation and coarse modes of the aerosol size distribution are well separated in size, then fractions of accumulation or coarse-mode aerosols to the total, with respect to number or volume (mass) will be significantly different. In cases, where both the modes are closer (i.e., closer to the boundary, 1 μm), then fine fraction estimated with respect to number or volume will not differ significantly. This could be the reason for the slope close to 1.0, as seen in Figure 7. The good agreement, notwithstanding the above, provides a validation of MODIS retrieval over the land on the one hand, while indicating the columnar and near-surface properties to be well associated during the dry, winter period considered here. It also indicates the general temporal stability of the aerosol features over the campaign period. The temporal stability has also been examined independently in Figure 8, where we have plotted the standard deviation of AOD for the month of February 2004, estimated from the daily AOD values at 550 nm, from the MODIS data. It is clearly seen that the standard deviations are very small (<0.03) for most part of the study region except in two small isolated pockets around the urban center, Hyderabad. This corroborates the observations deduced from Figures 6a and 6b) and adds to the general validity of our assumption that the period of study has very low temporal variation in aerosol properties. It is also worth mentioning that the points that showed larger deviation from the mean line (Figure 7) corresponded generally to the cases when the four MODIS grid points around our observation location showed largely differing values among themselves, implying the prevalence of a significant spatial heterogeneity in that region.

4.4. Spatial Variation of Number Size Distribution

[39] Number size distributions are important inputs in the study of effect of aerosols on atmospheric processes and in estimating radiative forcing [*Penner et al.*, 2001]. They are also vital inputs in estimating extinction coefficients and hence the aerosol optical depth. Number size distributions (nsd) were retrieved from the QCM measurements (by converting the mass size distributions to number size distributions using the same value of aerosol density). The uncertainty in this is discussed in section 3. Then the mean nsd is estimated for each location by averaging the instantaneous measurements. In most of the locations the nsd is found to decrease monotonically with size except at a few locations along the west coast and the inland forested regions where a clear bimodality was seen with a coarse mode at ~1.5 μm. As the limited number of size channels in the QCM did not facilitate parameterizing the nsds with a multimodal distribution, they were approximated to the inverse power law form

$$nsd = \frac{dn}{dr} = Cr^{-\nu}, \tag{6}$$

where C is a constant and ν is the aerosol size index. The spatial variation of the index ν is shown in Figure 9, which shows ν to vary, in general, from 3.5 to 5.0 and its spatial variation resembles that of A_f (Figure 6a). However, unlike the high A_f, which is spread on a wider region in the eastern part in Figure 6a, high ν (in Figure 9) is confined to a narrow region. Nevertheless, the results are consistent and relatively high values of ν (>4.5) occur in the coastal and the adjacent inland regions where A_f was >~0.65. In contrast to this, over the semiarid and plateau regions the size index was lower. To examine the differences in the

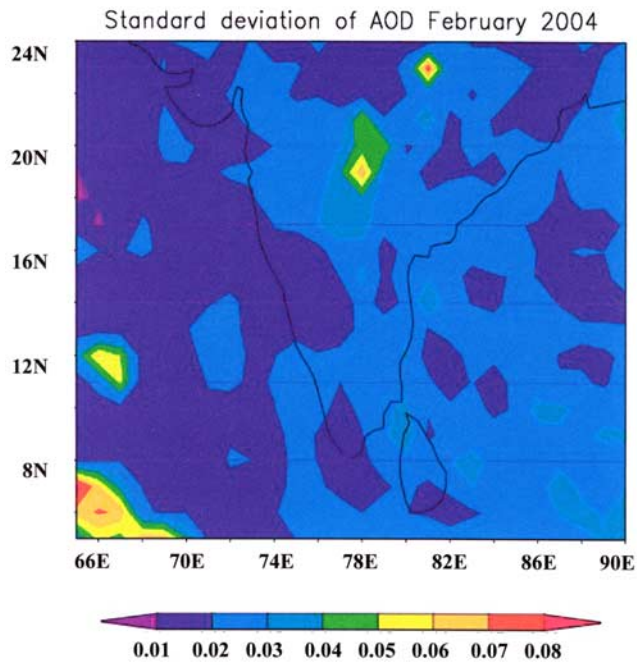

Figure 8. Spatial variation of the standard deviation of (AOD) at 550 nm, estimated from the daily aerosol optical depth (AOD) values from MODIS data for February 2004. Note the low values of the standard deviation for most of the study region.

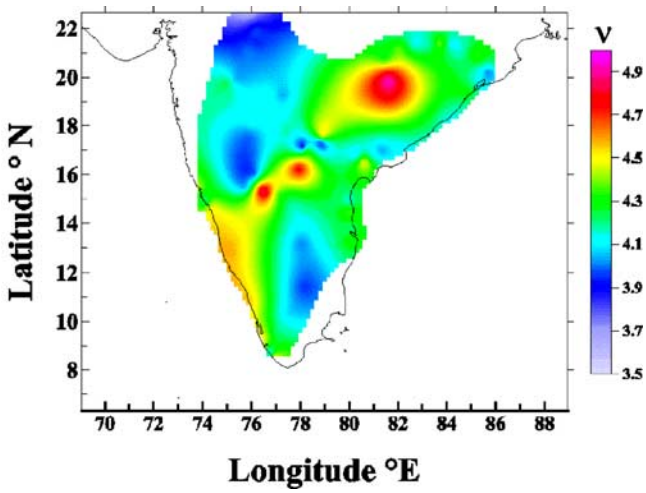

Figure 9. Spatial variation of aerosol size index.

aerosol size indices between urban and nonurban areas, the size indices retrieved for the urban areas were grouped together and averaged. These indices ranged from 4.3 to 5.1 with an average value of 4.5 ± 0.1. For the nonurban (remote) areas, the size indices ranged from 3.9 to 4.5, with an average value of 4.2 ± 0.02. This shows that the size spectra over urban areas are relatively steeper indicating abundance of fine particles, which could be locally produced. The absence of these local sources, along with the microphysical processes (like coagulation) taking place during aging of the aerosols would be causing the flattening of the size spectra in nonurban areas, in the accumulation regime.

5. Summary and Conclusions

[40] An intense field campaign for generating a spatial composite of aerosol characteristics over peninsular India was made and collocated measurements of the mass concentration and size distribution of near-surface aerosols were made onboard instrumented vehicles along the road network during the dry, winter season (February–March) of 2004.

[41] Spatial variation of aerosol mass concentration showed generally high values (50 to 80 $\mu g\ m^{-3}$) along the coastal regions and a low (<30 $\mu g\ m^{-3}$) in the interior continental regions.

[42] Hot spots of high aerosol mass concentration (>60 $\mu g\ m^{-3}$) are observed around coastal, industrialized and urban areas. The high population density (~70% of the more than 1 billion population of India lives in the coastal belt, extending over 7500 km and the study region covered a major part of the Indian coastline) and the consequent anthropogenic impact, increased RH and the shallow boundary layer all contribute to this enhancement.

[43] Accumulation-mode aerosols contributed more than 60% of the total aerosol mass concentration at coastal locations, while it is seen to be about 40% over the interior semi arid continental regions. The spatial composite of accumulation-mode share to the total aerosol concentration, agreed very well with the monthly mean spatial composite of aerosol fine-mode fraction deduced from MODIS data for the study region. A point by point comparison yielded a linear association with a slope of 1.09 and correlation coefficient of 0.79.

[44] Mass concentration obtained from different QCMs, and the QCM and HVS, agreed within ~20%. Spatial variation of aerosol size index resembles that of accumulation-mode fraction and varies from 3.5 to 5.0.

[45] **Acknowledgments.** The experiment formed part of the Land Campaign conducted under the ISRO-GBP. We acknowledge J. Srinivasan for mooting the idea of land campaign, Shyam Lal (the campaign coordinator), the ISRO-GBP program office, as well as the staff of NRSA station, Shadnagar, for all the help received during this work. The NCEP/NCAR reanalysis is provided by the NOAA-CIRES Climate Diagnostics Center, Boulder, Colorado from their website http://www.cdc.noaa.gov.

References

Bates, T. S., B. J. Huebert, J. L. Gras, F. B. Griffiths, and P. A. Durkee (1998), International Global Atmospheric Chemistry (IGAC) Project's First Aerosol Characterization Experiment (ACE1): Overview, *J. Geophys. Res.*, *103*, 16,297–16,318.

Boucher, O., and T. L. Anderson (1995), GCM assessment of the sensitivity of direct climate forcing by anthropogenic sulphate aerosols to aerosol size and chemistry, *J. Geophys. Res.*, *100*, 26,117–26,134.

Bukowiecki, N., J. Dommen, A. S. H. Prevot, R. Richter, E. Weingartner, and U. Baltensperger (2002), A mobile pollutant measurement laboratory—Measuring gas phase and aerosol ambient concentrations with high spatial and temporal resolution, *Atmos. Environ.*, *36*, 5569–5579.

Charlson, R. J., and H. Rodhe (1982), Factors controlling the acidity of natural rain water, *Nature*, *295*, 683–685.

Charlson, R. J., S. E. Schwartz, J. M. Hales, R. D. Cess, J. A. Coakley, J. E. Hansen, and D. J. Hoffmann (1992), Climate forcing by anthropogenic aerosols, *Science*, *255*, 423–430.

Dingenen, R. V., et al. (2004), A European aerosol phenomenology—1: Physical characteristics of particulate matter at kerbside, urban, rural and background sites in Europe, *Atmos. Environ.*, *38*, 2561–2577.

Gouriou, F., J.-P. Morin, and M.-E. Weill (2004), On-road measurements of particle number concentrations and size distributions in urban and tunnel environments, *Atmos. Environ.*, *38*, 2831–2840.

Hanel, G. (1976), The properties of atmospheric aerosol particles as functions of the relative humidity at thermodynamic equilibrium with the surrounding moist air, *Adv. Geophys.*, *19*, 73–188.

Huebert, B. J., T. Bates, P. B. Russell, G. Shi, X. J. Kim, K. Kawamura, G. Carmichael, and T. Nakajima (2003), An overview of ACE-Asia: Strategies for quantifying the relationships between Asian aerosols and their climatic impact, *J. Geophys. Res.*, *108*(223), 8633, doi:10.1029/2003JD003550.

Jayaraman, A. (1999), Results on direct radiative forcing of aerosols obtained over the tropical Indian Ocean, *Curr. Sci.*, *76*, 924–930.

Kalnay, E., et al. (1996), The NCEP/NCAR 40-year reanalysis project, *Bull. Am. Meteorol. Soc.*, *77*, 437–471.

Kaufman, Y. J. (1998), Smoke, Clouds and Radiation-Brazil (SCAR-B) experiment, *J. Geophys. Res.*, *103*, 31,783–31,808.

Kaufman, Y. J., D. Tanre, L. A. Remer, E. F. Vermote, A. Chq, and B. N. Holben (1997), Operational remote sensing of tropospheric aerosol over land from EOS moderate resolution imaging spectroradiometer, *J. Geophys. Res.*, *102*(D14), 17,051–17,067.

Kunhikrishnan, P. K., K. S. Gupta, R. Ramachandran, W. J. Prakash, and K. N. Nair (1993), Study on thermal internal boundary layer structure over Thumba, India, *Ann. Geophys.*, *11*, 52–60.

Lelieveld, J., et al. (2001), The Indian Ocean experiment: Widespread air pollution from south and Southeast Asia, *Science*, *291*, 1031–1035.

Momin, G. A., P. S. P. Rao, P. D. Safai, K. Ali, M. S. Naik, and A. D. Pillai (1999), Atmospheric aerosol characteristic studies at Pune and Thiruvananthapuram during INDOEX programme 1998, *Curr. Sci.*, *76*, 985–989.

Moorthy, K. K., B. V. K. Murthy, and P. R. Nair (1993), Sea-breeze front effects on boundary layer aerosols at a tropical station, *J. Appl. Meteorol.*, *32*, 1196–1205.

Moorthy, K. K., A. Saha, B. S. N. Prasad, K. Nirajan, D. Jhurry, and P. S. Pillai (2001), Aerosol optical depths over peninsular India and adjoining oceans during the INDOEX campaigns: Spatial, temporal and spectral characteristics, *J. Geophys. Res.*, *106*, 28,539–28,554.

Moorthy, K. K., P. S. Pillai, and S. S. Babu (2003), Influence of changes in the prevailing synoptic conditions on the response of aerosol characteristics to land/sea breeze circulations at a coastal station, *Boundary Layer Meteorol.*, *108*, 145–161.

Moorthy, K. K., S. S. Babu, S. V. Sunilkumar, P. K. Gupta, and B. S. Gera (2004), Altitude profiles of aerosol BC, derived from aircraft measurements over an Inland urban location in India, *Geophys. Res. Lett.*, *31*, L22103, doi:10.1029/2004GL021336.

Parameswaran, K., S. V. Sunilkumar, K. Rajeev, P. R. Nair, and K. K. Moorthy (2004), Boundary layer aerosols at Trivandrum tropical coast, *Adv. Space Res.*, *34*(4), 838–844, doi:10.1016/Jasr.2003.08.059.

Penner, J. E. et al. (2001), Aerosols, their direct and indirect effects, in *Climate Change 2001: The Scientific Basis*: *Contribution of Working Group I to the Third Assessment Report of the Intergovernmental Panel on Climate Change*, edited by J. T. Houghton et al., pp. 291–348, Cambridge Univ. Press, New York.

Pillai, P. S., and K. K. Moorthy (2001), Aerosol mass-size distributions at a tropical coastal environment: Response to mesoscale and synoptic processes, *Atmos. Environ.*, *35*, 4099–4112.

Pillai, P. S., S. S. Babu, and K. K. Moorthy (2002), A study of PM, PM10 and PM2.5 concentration at a tropical coastal station, *Atmos. Res.*, *61*, 149–167.

Pruppacher, H. R., and J. D. Klett (1978), *Microphysics of Clouds and Precipitation*, 714 pp., Springer, New York.

Raes, F., T. Bates, F. Mc Govern, and M. V. Liedekerke (2000), The 2nd Aerosol Characterisation Experiment (ACE-2): General overview and main results, *Tellus, Ser. B*, *52*, 111–125.

Ramanathan, V., et al. (2001), The Indian Ocean experiment: An integrated analysis of the climate forcing and effects of the great Indo-Asian haze, *J. Geophys. Res.*, *106*, 28,371–28,398.

Russell, B. P., P. V. Hobbs, and L. L. Stove (1999), Aerosol properties and radiative effect in the United States East Coast haze plume: An overview of the Tropospheric Aerosol Radiative Forcing Observational Experiment (TARFOX), *J. Geophys. Res.*, *104*, 2213–2222.

Smirnov, A., B. N. Holben, T. F. Eck, O. Dubovik, I. Slustsker, B. Chatenet, and R. T. Pinker (2002), Diurnal variability of aerosol optical depth observed at AERONET (Aerosol Robotic Network) sites, *Geophys. Res. Lett.*, *29*(23), 2115, doi:10.1029/2002GL016305.

Väkevä, M., K. Hämeri, T. Puhakka, E. D. Nilsson, H. Holiti, and J. M. Mäkelä (2000), Effects of meteorological processes on aerosol particle size distribution in an urban background area, *J. Geophys. Res.*, *105*, 9807–9821.

Weijers, E. P., A. Y. Khlystov, G. P. A. Kos, and J. W. Erisman (2004), Variability of particulate matter concentrations along roads and motorways determined by a moving measurement, *Atmos. Environ.*, *38*, 2993–3002.

Y. N. Ahmed, K. Narasimhulu, K. Ramgopal, and R. R. Reddy, Department of Physics, Sri Kirshnadevaraya University, Anantapur 515003, India. (rajururreddy@yahoo.co.uk)

K. V. S. Badarinath, T. R. Kiranchand, and K. M. Latha, Forestry and Ecology Division, National Remote Sensing Agency, Balanagar, Hyderabad 500037, India. (badrinath_kvs@nrsa.gov.in)

P. S. Brahmanandam, K. Niranjan, and B. M. Rao, Department of Physics, Andhra University, Visakhapatnam 530003, India. (niranjankandula@hotmail.com)

K. K. Moorthy, P. R. Nair, K. Parameswaran, P. S. Pillai, and S. V. Sunilkumar, Space Physics Laboratory, Vikram Sarabhai Space Centre, Trivandrum 695022, India. (krishnamoorthy_k@vssc.org)

A. Saha, Aryabhatta Research Institute for Observational Sciences, Manora Peak, Nainital, Uttaranchal 263129, India. (auromeet@upso.ernet.in)

S. K. Satheesh and V. Vinoj, Centre for Atmospheric and Oceanic Sciences, Indian Institute of Sciences, Bangalore 560 012, India. (satheesh@caos.iisc.ernet.in)